

## Cerium Oxide nanoparticles: Biosynthesis, Cytotoxic and UV protection

Abdolhossein Miri<sup>1</sup>, Honeyeh Beiki<sup>1</sup>, Mina Sarani<sup>2,\*</sup>

<sup>1</sup>Department of Pharmacognosy, Faculty of Pharmacy, Zabol University of Medical Sciences, Zabol, Iran

<sup>2</sup>Zabol Medicinal Plants Research Center, Zabol University of Medical Sciences, P.O. Box, 3333-669699, Zabol, Iran

**\*Corresponding author:** Mina Sarani

Zabol Medicinal Plants Research Center, Zabol University of Medical Sciences, P.O. Box, 3333-669699, Zabol, Iran.

Email: [minasarani64@gmail.com](mailto:minasarani64@gmail.com); [m.sarani@zbmu.ac.ir](mailto:m.sarani@zbmu.ac.ir)

### Abstract

In recent years, the nanoparticles applications have been well recognized in various fields. It is known that nanoparticles as an active ingredient in sunscreens are widely used. Zinc oxide and titanium oxide nanoparticles are common nanoparticles utilized in sunscreens. In this study, we aimed to suggest new nanoparticles for this purpose. Cerium oxide nanoparticles (CeO<sub>2</sub>-NPs) were synthesized by using *Musa sapientum* fruit peel extract. Synthesized nanoparticles were identified through Raman, Powder X-ray Diffraction (PXRD), Fourier Transform Infrared spectroscopy (FT-IR), Field Energy Scanning Electron Microscopy (FESEM) and Energy-Dispersive Spectroscopy (EDX). The results showed that size of synthesized nanoparticles are in range 4-13 nm. The cytotoxic activity of synthesized nanoparticles on lung (A549) cancer cell line was performed through MTT assay. The results showed that synthesized nanoparticles are non-toxicity against A549 cell line to below 500 µg/mL of nanoparticles concentration. The Sun protection factor (SPF) was estimated ~ 40 for synthesized CeO<sub>2</sub>-NPs. So, synthesized nanoparticles can be a good option for use in the cosmetics industry.

**Keywords:** CeO<sub>2</sub>-NPs, *Musa sapientum*, A549, MTT assay UV protection.

## 1. Introduction

Cerium is a lanthanide element with atomic number of 58 which has two oxide forms including cerium dioxide ( $\text{CeO}_2$ ) and di-cerium trioxide ( $\text{Ce}_2\text{O}_3$ ) [1-3]. These forms can convert to each other's. The cerium oxide are suitable for many industrial applications due to the exchange of  $\text{Ce}^{3+}$  and  $\text{Ce}^{4+}$  ions and the presence of oxygen holes in its crystalline structure [4]. Hence, this material is widely used in the glass industry, the manufacture of alloys and catalysts [5-7]. It can also act as UV absorber due to its large band-gap ( $\sim 4$  eV) [8].

Studies show the penetration of UV radiation into deep layers of the skin in a long time irritate and damage skin, and also it can lead to cancer. Irregularities of skin color, wrinkles and freckle are other complications of exposure of UV radiation. The sunscreen production industry has billions dollars per year turnover; so preparation more effective sunscreens with less skin stimulation, more transparent, and without changing appearance of consuming people is a demand of bazar [9-11]. To solve this problem, nanotechnology researchers have done studies. The results of these studies showed that titanium oxide ( $\text{TiO}_2$ ) and zinc oxide ( $\text{ZnO}$ ) nanoparticles have the potential to improve the performance of sunscreens. Newer studies have shown that  $\text{CeO}_2$ -NPs have a better ability than  $\text{ZnO}$  for utilization in sunscreens as absorption of UV rays [12].

Cancer is a disease in which abnormal cells were proliferated uncontrollably and can involve nearby tissues. This can occur following several genetic events, including inactivation of tumor suppressor genes and activation of oncogenes [13]. Today, various methods of surgery, chemotherapy and radiation therapy are used to treat cancer, but one of the disadvantages and side effects of these methods is the destruction of healthy cells. This has led researchers to move toward the new treatments with reducing side effects [14,15]. Nanotechnology can provide a tool for direct targeting, selective cancer cells, and increasing effectiveness for doctors [16]. Nanoparticles are used in a variety of ways, such as delivering drugs to cancer cells, as well as for imaging cancer cells and observing them more closely, and are well used for the diagnosis and treatment of cancer [17]. One of these nanoparticles is cerium oxide nanoparticles. Recent studies have shown that this nanoparticle has cytotoxic effect on cancer cells; therefore, further studies are important to determine the side effects and its use in the treatment of cancers [18].

Synthetic methods of nanoparticles play an important role in determining their size, morphology and properties. Metal oxide nanoparticles are generally synthesized using physical and chemical methods such as spray pyrolysis, ultrasonication, chemical evaporation and sol-gel [19-22]. Physical methods have limitations such as non-uniformity in particle size and expensive equipment. Metal oxide nanoparticles can be chemically synthesized by oxidation-reduction reactions or precipitation of required metal ion precursor in an aqueous solution phase [23,24].

Today, biosynthesis of nanoparticles considers by researchers because of their cost-effectiveness, environmentally friendly, faster, simple protocols, and mild reaction conditions. This method includes different biomaterials such as bacteria, fungi and plants as stabilizing and reducing agents. The nanoparticles biosynthesis is not unusual process in nature because some prokaryotes and eukaryotes are capable to produce of nanomaterials through intracellular and extracellular processes [25]. Biosynthesis methods can reduce the toxicity of produced nanomaterial, and produced nanoparticles have variety sizes and morphology [26-31].

*Musa sapientum* is belonging to Musaceae family. It is a plant with 6-8 meters height, and including helical and spiral shape of leaves. Its origin is Southeast Asia and well grows in humid tropics. *M. sapientum* are rich in potassium. Every part of it has pharmaceutical value, and includes a number of pharmaceutical compounds, such as sterol fatty acid, linoleic acid, fructose, xylose, galactose, glucose, mannose, and oleic acid. Also peel of *M. sapientum* having anthocyanins, carotenoids, phenolic compounds, amine compounds [32]. So, non-toxicity of nanoparticles is very important for application in industry and other fields. Hence, in this study, cerium oxide nanoparticles ( $\text{CeO}_2$ -NPs) was synthesized using *Musa sapientum* fruit peel extract and survey its cytotoxicity and sunscreen properties.

## **2. Experimental**

### **2.1. Synthesis of $\text{CeO}_2$ -NPs**

The dried and crushed *Musa sapientum* fruit peel was extracted using water as a solvent (ratio to 1:10) through the soaking method. In the next step results was filtered and filtrate was used for the synthesis of nanoparticles. 10 mL of the extract was diluted with 40 mL distilled water; then 50 mL of 0.05 M cerium nitrate was added in it. The solution was stirred at 70 °C

for 4 h and then it was dried in 90 °C. The resulting powder was sintered at 300, 400, 500 and 600 °C, separately. Obtained yellow powder was CeO<sub>2</sub>-NPs. The schematic diagrams of the synthesis of CeO<sub>2</sub>-NPs are shown in Figure 1.

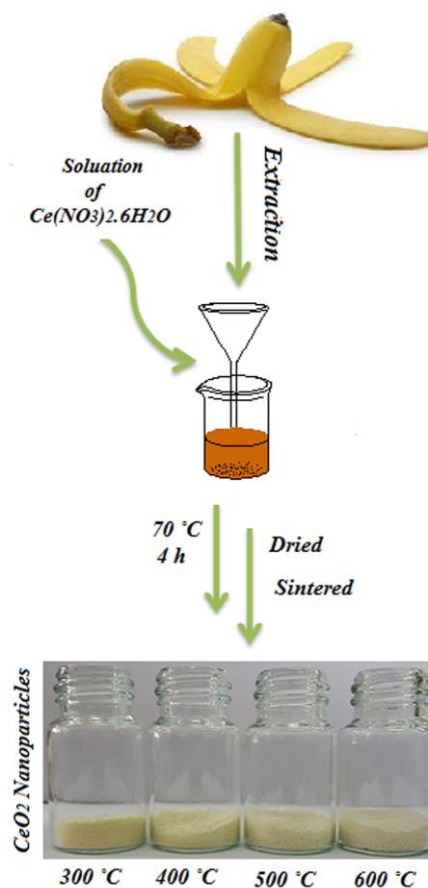


**Figure 1.** Schematic diagrams of the synthesis of CeO<sub>2</sub>-NPs using extract of *M. sapientum* fruit peel at four temperatures

## 2.2. Cytotoxicity evaluation of CeO<sub>2</sub>-NPs

The lung cancer cell line (A549) was prepared from Pasteur Institute of Iran. Cells were incubated in RPMI culture medium supplemented with 10% FBS, 100 µg/ml of Streptomycin, and 100 U/ml of Penicillin, at 37 °C and CO<sub>2</sub> atmosphere with 5% moisture. The cytotoxicity of synthesized CeO<sub>2</sub>-NPs was surveyed through 3-(4,5-Dimethylthiazol-2-yl)-2,5-diphenyltetrazolium bromide (MTT). For this purpose, 200 µl of cell suspension was poured to wells (1x10<sup>4</sup> Cell/well) tissue culture plate and incubated for 24 h. After that, 50 µl of synthesized CeO<sub>2</sub>-NPs (0-500 µg/ml, separately) were added into each well and again incubated for 24 h. Cell suspension with culture medium marked as control. MTT solution was prepared to add 5 mg/ml MTT dye in PBS buffer, and then 20 µl of this solution was

poured to each well of plate, and incubated for 3 h at 37 °C. At the end of, DMSO (100 µl) was added to each well and optical absorbance of each well was measured at 570 nm by using a micro-plate reader. Cell viability was presented as a percent compared to untreated control cells.

### 2.3. Sun Protection Factor (SPF) assay

SPF was matured using spectrophotometry method [33]. The solution of 100, 1000 and 10000 ppm of synthesized nanoparticles at four sintered temperature was prepared using ethanol as a solvent, and their absorbance were measured at 290 to 320 nm.

### 2.3. Characterization

Structure, morphology and size of synthesized CeO<sub>2</sub>-NPs were identified through Raman (Takram P50C0R10 model in 532 nm laser wave length), Powder X-ray Diffraction (PXRD, X'Pert PRO MPD PANalytical model, Netherlands), Fourier Transform Infrared spectroscopy (FT-IR, Bruker Tensor27) and Field Energy Scanning Electron Microscopy (FESEM, TESCAN model of MIRA3) methods.

## 3. Discussion and conclusion

The phenolic compound of *Musa sapientum* fruit peel can act as a reducing and stabilizer agent for cerium ions. Then oxidation transfer between Ce<sup>+3</sup> to Ce<sup>+4</sup> simultaneously accomplished due to oxygen of air, which leads to CeO<sub>2</sub>-NPs product. Figure 2 shows PXRD pattern of the synthesized CeO<sub>2</sub>-NPs using aqueous extract of *M. sapientum* fruit peel at 300, 400, 500 and 600 °C. Accordance with JCPDS standard, all appearing peaks in diffraction pattern confirm the structure of fluorite cubic structure for synthesized nanoparticles [34]. Size of synthesized nanoparticles at 300, 400, 500 and 600 °C were estimated by using the Scherrer equation ( $D=0.9*\lambda/\beta\cos\theta$ ; where  $\lambda$  is the X-ray wavelength,  $\beta$  is the full width at half the maximum (FWHM) and  $\theta$  is the Bragg's angle) [33], as 4.22, 5.25, 7.72 and 12.78 nm respectively, The results show with increasing sintering temperature, the particles size grow.

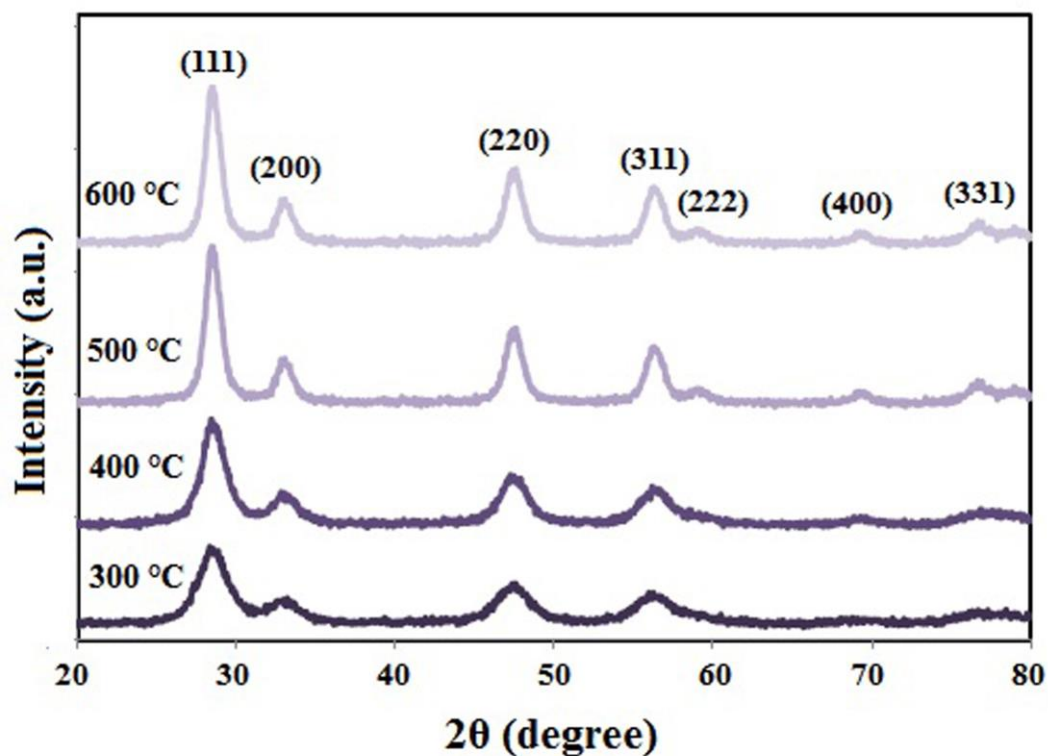


**Figure 2.** PXRD spectra of synthesized CeO<sub>2</sub>-NPs using extract of *M. sapientum* fruit peel at four temperatures

The Raman spectrum of the synthesized CeO<sub>2</sub>-NPs is shown in Figure 3 at 400 °C. This data illustrate structural irregularities and sample topologies [34]. The active Raman mode for synthesized CeO<sub>2</sub>-NPs shows a very strong band at 453 cm<sup>-1</sup>, which it conforms to F2g mode. The crystalline fluorite cubic structure confirms for synthesized nanoparticles [35].

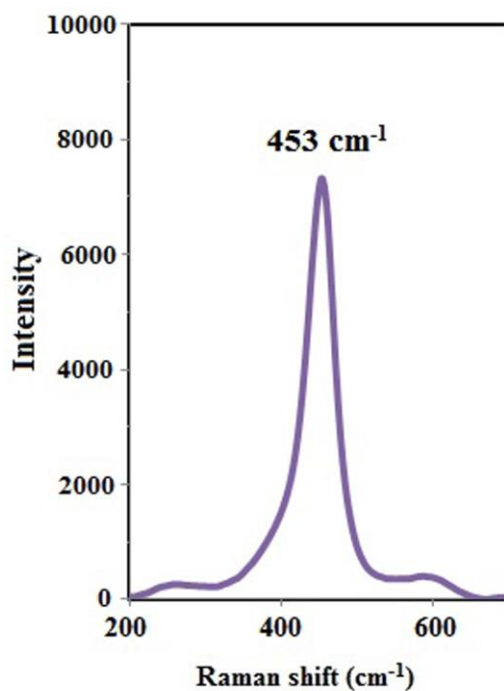


**Figure 3.** Raman spectrum of synthesized CeO<sub>2</sub>-NPs using extract of *M. sapientum* fruit peel at 400 °C

The FESEM image of synthesized nanoparticles at 400 °C is shown in Figure 4A. The appearance of synthesized particles is snowflakes, and the grading particles are not well defined, it is foam-like. This issue may be due to CO<sub>2</sub> and H<sub>2</sub>O fast exit from raw martial during calcination presses [36, 37]. Figure 4B shows EDX graph of synthesized nanoparticles at 400 °C. The percent of cerium and oxygen is 22.05 and 77.59, which it shows only present of cerium and oxygen elements in synthesized sample.

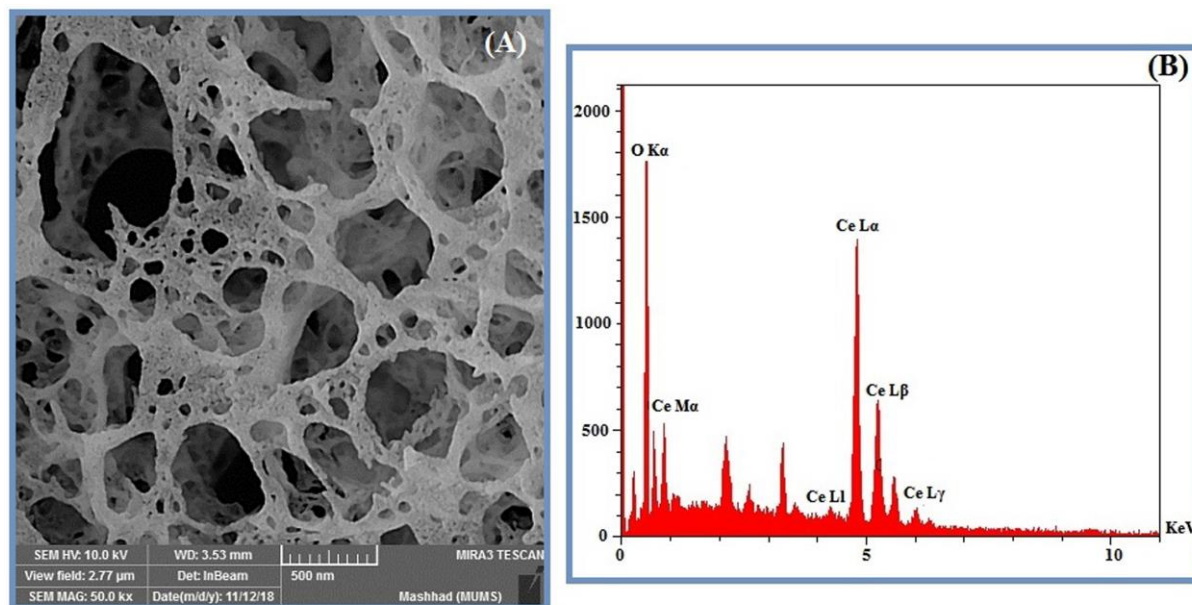


**Figure 4.** (A) FESEM image, (B) EDX graph of synthesized CeO<sub>2</sub>-NPs using extract of *M. sapientum* fruit peel at 400 °C.

The cytotoxic activity of synthesized CeO<sub>2</sub>-NPs was survey by using *M. sapientum* extract on lung (A549) cancer cell lines. It performed through MTT assay and based on transformation of solvable tetrazolium salt to unsolvable formazan through mitochondria of living cells. As shown in Figure 5, this test was performed in 0-500 μg/ml of concentrations of synthesized nanoparticles after 24 h treatment time. The results presented that cell viability is 70 % in 500 μg/ml of nanoparticles concentration. Here, synthesized CeO<sub>2</sub>-NPs by using *M. sapientum* extract were not cytotoxic at concentrations under 500 μg/mL. The same results show for synthesized CeO<sub>2</sub>-NPs by using *P. fracta* [33], gum [38], agarose [39] against HT-29, Nero2A and L929 cell lines, respectively. So, synthesized nanoparticles can utilize for applications such as drug delivery, cosmetic and ceramics.



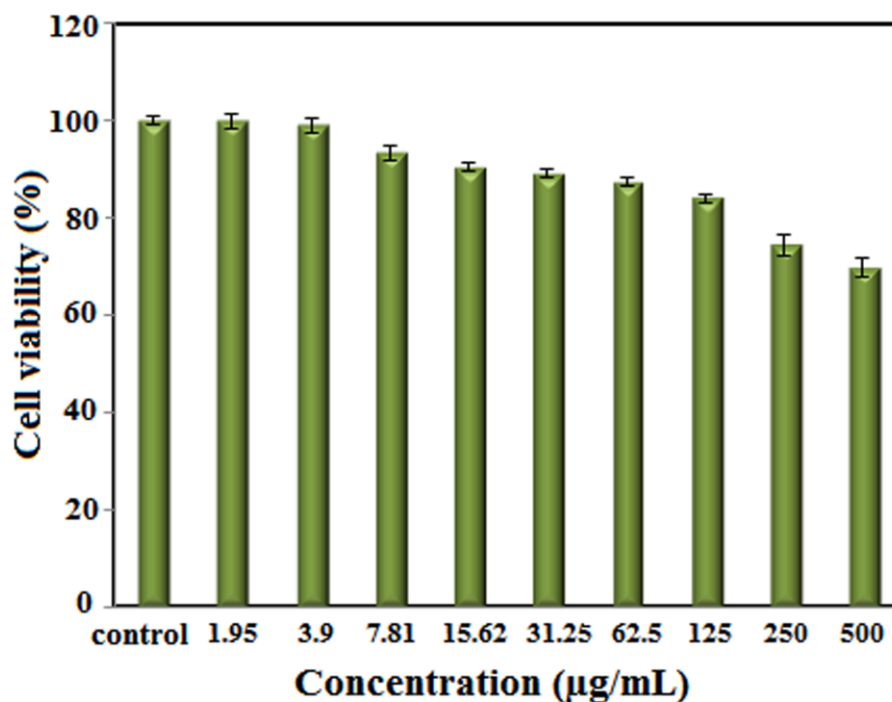


**Figure 5.** Cell viability of synthesized CeO<sub>2</sub>-NPs on A549 cell line after 24 h incubation.

Today, there are over 300 sunscreens containing zinc oxide and titanium oxide nanoparticles in the market [40]. Previous studies have shown that CeO<sub>2</sub>-NPs have a better ability to absorb UV than to zinc oxide nanoparticles [12]. The sun protective factor of synthesized nanoparticles was calculated through the Mansur *et al* equation (Eq. 1) [40].

$$\text{SPF} = \text{CF} \times \sum_{290}^{320} \text{EE}(\lambda) \times I(\lambda) \times \text{Abs}(\lambda) \quad \text{Eq. 1}$$

Where, CF=10 (Optimization factor),  $\text{EE}_{\lambda}$  is Erythemal effect of radiation at wavelength  $\lambda$ ,  $I_{(\lambda)}$  is intensity of sunlight at wavelength  $\lambda$ ,  $\text{abs}_{(\lambda)}$  is absorption of wavelength  $\lambda$  by test solution. The values for the  $\text{EE}(\lambda)$ ,  $I(\lambda)$  determine by Sayre *et al* that insert in Table 1.

**Table 1.** Normalized product function used in the calculation of SPF

Wavelength (nm)	290	295	300	305	310	315	320
EE × I	0.0150	0.0817	0.2874	0.3278	0.1864	0.0839	0.0180

The SPF values of synthesized CeO<sub>2</sub>-NPs (1 gr in 100 mL ethanol) at 300, 400, 500 and 600 °C calculate 38.76, 26, 26.30 and 11.08, respectively (Table 2). As shown in Figure 6, UV

protection values of synthesized nanoparticles reduce by reducing the particle size. The particle size is an important factor for adsorption and transmission of UV ray. So reducing the particles size reduces the distance between them, so the light is more refracted towards its path. The synthesized CeO<sub>2</sub>-NPs have different sizes at four temperatures, and analytic of SPF results showed that SPF levels increased as the particle size gets smaller. The synthesized CeO<sub>2</sub>-NPs have a good ability to absorb UV rays.

**Table 2.** SPF values of synthesized CeO<sub>2</sub>-NPs at four temperatures

Concentration of CeO <sub>2</sub> -NPs (mg/L)	SPF values			
	300 °C	400 °C	500 °C	600 °C
10000	38.76	26	26.30	11.08
1000	10.93	8.33	6.73	5.28
100	2.91	1.46	1.49	1.09

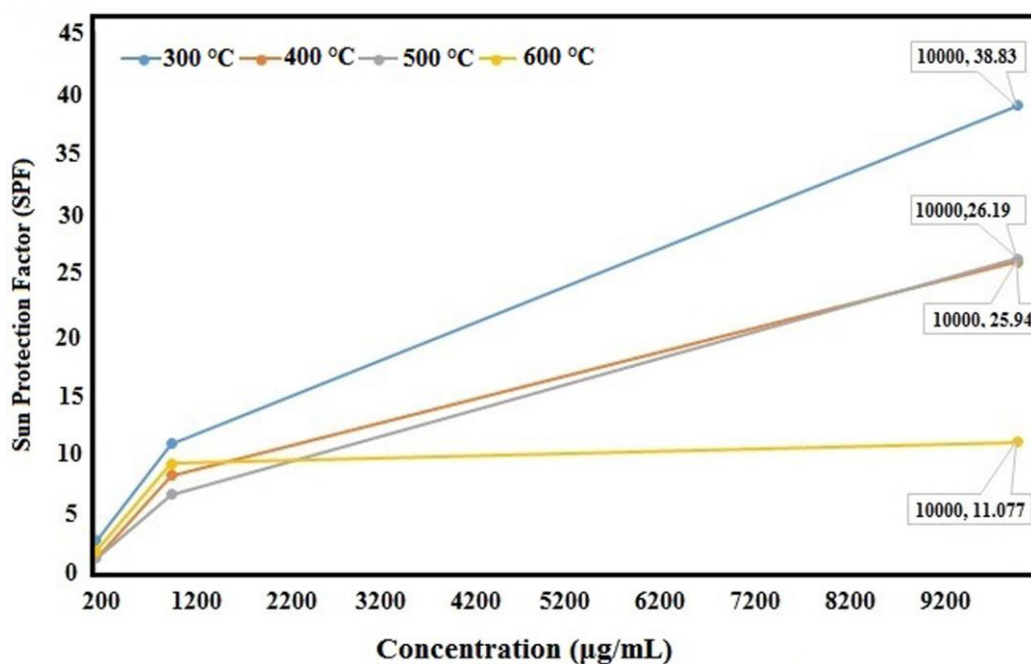


**Figure 6.** UV protection of synthesized CeO<sub>2</sub>-NPs using extract of *M. sapientum* fruit peel.

## Conclusion

Due to the importance of sunscreens in cosmetic products, efforts have been done to improve their quality by researchers. The results of the studies show that some nanoparticles have a good ability to absorb UV rays. CeO<sub>2</sub>-NPs can be suggested as an option for this purpose due to its high band-gap. These nanoparticles are synthesized through a quick and low-cost method using aqueous extract of *M. sapientum* peel. The size of synthesized nanoparticles was in the range of 4-13 nm. The cytotoxic study of synthesized nanoparticles show that they are non-cytotoxic on A549 cell line at below 500 µg/ml. So, synthesized nanoparticles are suitable for medicinal applications. The results of the SPF measurement of synthesized nanoparticles show that by decreasing the particle size, the SPF level increases.

## Compliance with ethical standards

Conflict of interest the authors declare that they have no conflict of interest.

## Ethical approval

This study was done on synthesis of CeO<sub>2</sub>-NPs by using extract of *M. sapientum* peel. In following, cytotoxic activity of synthesized nanoparticles was performed using MTT assay against lung (A549) cell line. The lung cell line was prepared from Pasteur Institute of Iran. Therefore, this research does not require the approval of Animal Experimentation Committee.

## References

1. C. Korsvik.; S. Patil.; S. Seal.; W.T. Self. Superoxide dismutase mimetic properties exhibited by vacancy engineered ceria nanoparticles. *Chem. Commun.* **2007**, *10*, 1056-1058.
2. X. Beaudoux.; M. Viro.; T. Chave.; G. Durand.; G. Leturcq.; S.I. Nikitenko. Vitamin C boosts ceria-based catalyst recycling. *Green.Chem.* **2016**, *18*, 3656-3668.
3. C. Xu.; X. Qu. Cerium oxide nanoparticle: a remarkably versatile rare earth nanomaterial for biological applications. *NPG Asia Mater.* **2014**, *6*, e90.
4. S. Das.; J.M. Dowding.; K.E. Klump.; J.F. McGinnis.; W. Self.; S. Seal. Cerium oxide nanoparticles: applications and prospects in nanomedicine. *Nanomedicine (Lond)*. **2013**, *8*, 1483-1508.
5. C.R. Stanek.; A.H.H. Tan.; S.L. Owens.; R.W. Grimes. Atomistic simulation of CeO<sub>2</sub> surface hydroxylation: implications for glass polishing. *J. Mater. Sci.* **2008**, *43*, 4157-4162.

6. S. Singh.; T. Dosani.; A.S. Karakoti.; A. Kumar.; S. Seal.; W.T. Self. A phosphate-dependent shift in redox state of cerium oxide nanoparticles and its effects on catalytic properties. *Biomaterials*. **2011**, *32*, 6745-6753.
7. W.M. AL-Shawafi.; N. Salah, A. Alshahrie.; Y.M. Ahmed.; S.S. Moselhy.; A.H. Hammad.; M.A. Hussain.; A. Memic. Size controlled ultrafine CeO<sub>2</sub> nanoparticles produced by the microwave assisted route and their antimicrobial activity. *J Mater Sci: Mater Med*. **2017**, *28*, 177.
8. J.J. Miao.; H. Wang.; Y.R. Li.; J.M. Zhu.; J.J. Zhu. Ultrasonic-induced synthesis of CeO<sub>2</sub> nanotubes. *J. Cryst. Growth*. **2005**, *281*, 525-529.
9. K. Morabito.; N.C. Shapley.; K.G. Steeley.; A. Tripathi. Review of sunscreen and the emergence of non-conventional absorbers and their applications in ultraviolet protection. *Int J Cosmet Sci*. **2011**, *33*, 385-390.
10. S. Kaul.; N. Gulati.; D. Verma.; S. Mukherjee.; U. Nagaich. Role of Nanotechnology in Cosmeceuticals: A Review of Recent Advances. *J Pharm*. **2018**, 19 pages.
11. B. Herzog.; M. Wehrle.; K. Quass. Photostability of UV Absorber Systems in Sunscreens. *Photochem Photobiol*. **2009**, *85*, 869-878.
12. T. Boutard.; B. Rousseau.; C. Couteau.; C. Tomasoni.; C. Simonnard.; C. Jacquot.; L.J.M. Coiffard.; K. Konstantinov.; T. Devers.; C. Roussakis. Comparison of photoprotection efficiency and antiproliferative activity of ZnO commercial sunscreens and CeO<sub>2</sub>. *Mater Lett*. **2013**, *108*, 13-16.
13. O. De Wever.; L. Lapeire.; A. De Boeck.; A. Hendrix. Cellular and molecular mechanisms of cancer cell invasion. *Verh K AcadGeneesk Belg*. **2010**, *72*, 309-26.
14. L.H. Stacey.; C. Nikki. Chemokine signaling in cancer: Implications on the tumor microenvironment and therapeutic targeting. *Cancer Ther*. **2009**, *7*, 254-267.
15. V. Golfopoulos.; G. Pentheroudakis.; N. Pavlidis. Treatment of colorectal cancer in the elderly: a review of the literature. *Cancer Treat Rev*. **2006**, *32*, 1-8.
16. A. Ediriwickrema.; W.M. Saltzman. Nanotherapy for Cancer: Targeting and Multifunctionality in the Future of Cancer Therapies. *ACS BiomaterSci Eng*. **2015**, *1*, 64-78.
17. A. Babu.; A.K. Templeton.; A. Munshi.; R. Ramesh. Nanodrug delivery systems: a promising technology for detection, diagnosis, and treatment of cancer. *AAPS PharmSciTech*. **2014**, *15*, 709-721.
18. S. Das.; J.M. Dowding.; K.E. Klump.; J.F. McGinnis.; W. Self.; S. Seal. Cerium oxide nanoparticles: applications and prospects in nanomedicine. *Nanomedicine (Lond)*. **2013**, *8*(9), 1483-508.
19. S. Rajeshkumar.; P. Naik. Synthesis and biomedical applications of cerium oxide nanoparticles-a review. *Biotechnol. Rep*. **2018**, *17*, 1-5.
20. P. Nazari.; S. Gharibzadeh.; F. Ansari.; B.A. Nejang.; M. Eskandari.; S. Kohnehpoushi.; V. Ahmadi.; M. Salavati-Niasari. Facile green deposition of nanostructured porous NiO thin film by spray coating. *Mater. Lett*. **2017**, *190*, 40-44.

21. R. Kumar.; Y. Diamant.; A. Gedanke. Sonochemical synthesis and characterization of nanometer-size transition metal oxides from metal acetates. *Chem. Mater.* **2000**, *12*, 2301-2305.
22. M. Darroudi.; M. Sarani.; R. Kazemi Oskuee.; A. Khorsand Zak.; H.A. Hosseini.; L. Gholami. Green synthesis and evaluation of metabolic activity of starch mediated nanoceria. *Ceram. Int.* **2014**, *40*, 2041-2045.
23. P. Kumar Singh.; P. Kumar.; A. Kumar Das. Unconventional Physical Methods for Synthesis of Metal and Non-metal Nanoparticles: A Review. *Proc Natl Acad Sci, India, Sect A Phys Sci.* **2019**, *89*, 199-221.
24. C. Dhand.; N. Dwivedi.; X.J. Loh.; A.N.J. Ying.; N.K. Verma.; R.W. Beuerman.; R. Lakshminarayanan.; S. Ramakrishna. Methods and strategies for the synthesis of diverse nanoparticles and their applications: a comprehensive overview. *RSC Adv.* **2015**, *5*, 105003-105037.
25. K.B. Narayanan.; N. Sakthivel. Green synthesis of biogenic metal nanoparticles by terrestrial and aquatic phototrophic and heterotrophic eukaryotes and biocompatible agents. *Adv. Colloid Interface Sci.* **2011**, *169*, 59-79.
26. A. Miri.; H.O. Shahraki Vahed.; M. Sarani. Biosynthesis of silver nanoparticles and their role in photocatalytic degradation of methylene blue dye. *Res Chem Intermediat.* **2018**, *44*, 6907-6915.
27. A. Miri.; S.R. Mousavi.; M. Sarani. Using *Biebersteinia multifida* Aqueous Extract, the Photocatalytic Activity of Synthesized Silver Nanoparticles. *OJC.* **2018**, *34(3)*, 1513-1517.
28. A. Miri.; M. Sarani. Biosynthesis and Cytotoxic Study of Synthesized Zinc Oxide Nanoparticles Using *Salvadora persica*. *BioNanoScience.* **2019**, *9*, 164-171.
29. M. Khatami.; H.Q. Alijani.; M. Haghghat.; M. Bamrovat.; S. Azhdari.; M. Ahmadian.; M. Nobre.; M.R. Heidari.; M. Sarani.; S. Khatami. Green Synthesis of Amorphous Iron Oxide Nanoparticles and their Antimicrobial Activity against *Klebsiella pneumonia*, *Pseudomonas aeruginosa* and *Escherichia coli*. *Iran J Biotechnol.* **2019**, *10*, 33-39.
30. M. Safaei.; M.M. Foroughi.; N. Ebrahimpoor.; S. Jahani.; A. Omidi.; M. Khatami. A review on metal-organic frameworks: Synthesis and Applications. *Trends Analyt Chem.* **2019**, *118*, 401-425.
31. M. Khatami.; R.S. Varma.; M.R. Heydari.; M. Peydayesh.; A. Sedighi.; H.A. Askari.; M. Rohani.; M. Baniasadi.; S. Arkia.; F. Seyedi.; S. Khatami. Copper Oxide Nanoparticles Greener Synthesis Using Tea and its Antifungal Efficiency on *Fusarium solani*. *Geomicrobiol J.* **2019**, 1-5.
32. M.Z. Imam.; S. Akter. *Musa paradisiaca* L. and *Musa sapientum* L.: A Phytochemical and Pharmacological Review. *J App Pharma Sci.* **2011**, *05*, 14-20.
33. A. Miri.; M. Sarani. Biosynthesis, characterization and cytotoxic activity of CeO<sub>2</sub> nanoparticles. *Ceram. Int.* **2018**, *44*, 12642-12647.
34. Y. Lee.; G. He.; A.J. Akey.; R. Si.; M. Flytzani-Stephanopoulos.; I.P. Herman. Raman Analysis of Mode Softening in Nanoparticle CeO<sub>2-δ</sub> and Au-CeO<sub>2-δ</sub> during CO Oxidation. *J Am Chem Soc.* **2011**, *133*, 12952-12955.

35. A. Arumugam.; C. Karthikeyan.; A.S.H. Hameed.; K. Gopinath.; S. Gowri.; V. Karthika. Synthesis of cerium oxide nanoparticles using *Gloriosa superba* L. leaf extract and their structural, optical and antibacterial properties. *Mater Sci Eng C*. **2015**, *49*, 408-415.
36. A.B. Sifontes.; G. Gonzalez.; J.L. Ochoa.; L.M. Tovar.; T. Zoltan.; E. Can˜ izales. Chitosan as template for the synthesis of ceria nanoparticles. *Mater Res Bull*. **2011**, *46*, 1794-1799.
37. T.N. Ravishankar.; T. Ramakrishnappa.; G. Nagaraju.; H. Rajanaika. Synthesis and Characterization of CeO<sub>2</sub> Nanoparticles via Solution Combustion Method for Photocatalytic and Antibacterial Activity Studies. *ChemistryOpen*. **2015**, *4*, 46-54.
38. M. Darroudi.; M. Sarani.; R. Kazemi Oskuee.; A. Khorsand Zak.; M.S. Amiri. Nanoceria: Gum mediated synthesis and in vitro viability assay. *Ceram Intern*. **2014**, *40*, 2863-2868.
39. H. Kargar.; F. Ghasemi.; M. Darroudi. Bioorganic polymer-based synthesis of cerium oxide nanoparticles and their cell viability assays. *Ceram Intern*. **2015**, *41*, 1589-1594.
40. M.M. Donglikar.; S.L. Deore. Sunscreens: A review. *Pharmacogn J*. **2016**, *8*, 171-179.